Journal of Engineering Mathematics **39:** 367–385, 2001.

The evolution of travelling waves from chemical-clock reactions

S. J. PREECE, J. BILLINGHAM AND A. C. KING
School of Mathematics and Statistics, University of Birmingham, Edgbaston, Birmingham B15 2TT, U.K.

Received 6 March 2000; accepted in revised form 22 August 2000

Abstract. A clock-reaction is a chemical reaction which gives rise to an initial induction period before a significant change in concentration of one of the chemical species occurs. In this paper the development of travelling waves from a particular class of inhibited autocatalytic clock-reactions is analysed. The numerical solutions show that, after the induction period, a propagating reaction-diffusion front is initiated. This front is seen to accelerate initially and then to become a constant-speed travelling wave. An asymptotic analysis of the large-time travelling-wave behaviour is given and from this it is possible to fix a minimum wave speed. The asymptotic predictions of the wave speed are found to agree well with those of the numerical solution.

Key words: clock-reaction, autocatalysis, inhibition, reaction-diffusion, travelling wave

1. Introduction

Propagating reaction-diffusion fronts were first considered by Luther [1] over 80 years ago and a mathematical formulation was first carried out by Fisher [2] and analysed in more detail by Kolmogorov *et al.* [3]. Since the work of Merkin and Needham [4] on a simple autocatalytic chemical system much research has been published relating to the development of travelling waves. In this paper we analyse the development, in an unstirred medium, of a class of reaction schemes which is known to give rise to clock-reaction behaviour and are able to demonstrate the existence of travelling waves.

A reaction is regarded as displaying clock characteristics if, after the initial mixing, a significant induction period is observed before a rapid change in one of the product or reactant concentrations occurs. Such reactions often give rise to observable phenomena at the end of the induction period. Examples of clock-reactions include the arsenic(III) sulfide clock-reaction [5], the formaldehyde clock-reaction [6], the iodine bisulphate clock [7] and the hydration of carbon dioxide [8]. In this paper we consider two mechanisms which can give rise to clock-reaction behaviour. The first is simple autocatalysis, which can be described as an induction reaction. An example of such a scheme is,

$$A + nB \longrightarrow (n+1)B, \qquad \text{rate } kab^n, \tag{1}$$

where lower-case letters denote the respective chemical concentrations and k is a reaction-rate constant. Examples of solution-phase reactions which are thought to be well modelled by cubic autocatalysis are the iodate-arsenous acid reaction [9] and the iodine-bisulphate clock-reaction [10, pp. 54–56]. Another mechanism which can lead to clock-reaction behaviour is,

$$\begin{aligned} P &\longrightarrow B, && \text{rate } k_0 p, \\ B + C &\longrightarrow D, && \text{rate } k_1 bc, \end{aligned}$$

which can be described as an inhibition reaction. The clock chemical, B, is supplied to the system via the decay of the precursor chemical P. An inhibitor chemical, C, reacts with the clock chemical limiting its concentration. Once the inhibitor chemical is consumed the concentration of the clock chemical starts to increase. This system has been analysed mathematically in a well stirred situation by Billingham and Needham [11]. Examples of reactions which are thought to be well modelled by this mechanism are the photosynthesis of hydrogen chloride inhibited by ammonia and the polymerisation of vinyl acetate by benzoquinone [12].

In this paper we analyse the behaviour of the system,

$$P \longrightarrow A, \qquad \text{rate } k_0 p, \tag{2}$$

$$A + nB \longrightarrow (n+1)B, \qquad \text{rate } k_1 a b^n, \tag{3}$$

$$mB + C \longrightarrow D, \qquad \text{rate } k_2 b^m c, \tag{4}$$

for the cases $n = m = 1, 2$. This system was first analysed by Billingham and Needham [13] who assumed the decay of the precursor to be negligible. Using asymptotic methods, they were able to obtain expressions for the length of the induction period in each case. Preece *et al.* [14] extended this work to allow for the consumption of the precursor chemical. They obtained modified expressions for the induction period and showed that clock-reaction behaviour was only observed within certain parameter limits.

In the first part of this paper numerical solutions are presented which show that, when a clock-reaction is initiated with localised initial conditions, the rapid growth in concentration of autocatalyst sets up a propagating reaction-diffusion front. After an initial transient phase in which the reaction front accelerates, a constant-speed travelling wave is seen to develop. Using asymptotic methods, we construct a large-time travelling-wave solution for the cases $n = m = 1, 2$ and are able to fix a minimum wave speed in each case. Our asymptotic predictions of wave speed are found to agree well with those of the numerical solution.

2. Mathematical formulation

We formulate the problem for $n = m = 1$ or 2 setting $m = n$ and choose to study the case of one-dimensional slab geometry with the diffusion coefficients of the chemical species equal. From reaction scheme (2), (3), (4) we obtain the partial differential equations,

$$\frac{\partial p}{\partial t} = D\frac{\partial^2 p}{\partial \bar{x}^2} - k_0 p, \tag{5}$$

$$\frac{\partial a}{\partial t} = D\frac{\partial^2 a}{\partial \bar{x}^2} + k_0 p - k_1 a b^n, \tag{6}$$

$$\frac{\partial b}{\partial t} = D\frac{\partial^2 b}{\partial \bar{x}^2} + k_1 a b^n - n k_2 b^n c, \tag{7}$$

$$\frac{\partial c}{\partial t} = D\frac{\partial^2 c}{\partial \bar{x}^2} - k_2 b^n c, \tag{8}$$

which are to be solved subject to the initial conditions,

$$\begin{aligned} p(\bar{x}, 0) &= p_0, \\ a(\bar{x}, 0) &= 0, \\ b(\bar{x}, 0) &= \begin{cases} b_0 & \bar{x} \le |l| \\ 0 & \bar{x} > |l|, \end{cases} \end{aligned} \tag{9}$$

$$c(\bar{x}, 0) = c_0.$$

These conditions describe an initially uniform concentration of precursor and inhibitor chemical and an initial top hat distribution of the autocatalyst of half width l. We impose no flux boundary conditions on all chemical species at infinity. As no spatial variation will occur in the precursor concentration, Equation (5) can be integrated to give

$$p = p_0 \mathrm{e}^{-k_0 t}. \tag{10}$$

We define dimensionless variables as

$$\alpha = a/b_0, \quad \beta = b/b_0, \quad \gamma = c/b_0, \quad \bar{x} = \left(\frac{k_1 b_0^n}{D}\right)^{1/2} x, \quad \tau = k_1 b_0^n t, \tag{11}$$

and Equations (6), (7) and (8) reduce to

$$\frac{\partial \alpha}{d\tau} = \frac{\partial^2 \alpha}{\partial x^2} + \mu \mathrm{e}^{-\epsilon_0 \delta \tau} - \alpha \beta^n, \tag{12}$$

$$\frac{\partial \beta}{d\tau} = \frac{\partial^2 \beta}{\partial x^2} + \alpha \beta^n - \frac{n}{\delta} \beta^n \gamma, \tag{13}$$

$$\frac{\partial \gamma}{d\tau} = \frac{\partial^2 \gamma}{\partial x^2} - \frac{1}{\delta} \beta^n \gamma, \tag{14}$$

where the parameters ϵ_0, δ and μ are defined as

$$\epsilon = \frac{k_0}{k_1 b_0^n}, \quad \delta = \frac{k_1}{k_2 b_0}, \quad \mu = \epsilon P_0, \quad \text{with} \quad P_0 = \frac{p_0}{b_0}. \tag{15}$$

These equations must be solved subject to the initial conditions

$$\begin{aligned} \alpha(x, 0) &= 0, \\ \beta(x, 0) &= \begin{cases} 1 & x < |\xi| \\ 0 & x > |\xi|, \end{cases} \\ \gamma(x, 0) &= \lambda, \end{aligned} \tag{16}$$

where,

$$\lambda = \frac{c_0}{b_0}, \quad \xi = \left(\frac{D}{k_1 b_0^n}\right)^{\frac{1}{2}} l. \tag{17}$$

P_0 and λ are the dimensionless initial concentrations of P and C, respectively. The parameters ϵ and $1/\delta$ are measures of the reaction rate of steps (2) and (4), respectively, relative to the rate of the autocatalytic step (3). The diffusion coefficient has been scaled out of the governing equations and we have retained the imposed length scale in the initial conditions via the parameter ξ. It has been shown by Billingham and Needham [13] that in a well stirred environment the length of the induction period is of $O(\delta^{-1})$ for the cases $n = 1, 2$. We choose to consider the small δ situation, in which

$$\epsilon = \epsilon_0 \delta \quad \epsilon_0 = O(1) \quad \text{as} \quad \delta \to 0 \quad \text{with} \quad \mu = O(1). \tag{18}$$

This ensures that the effect of precursor consumption is significant at the time of initiation of the reaction-diffusion front and produces interesting phenomena which are described in the next section.

3. Numerical solution

We now present a numerical solution of Equations (12), (13) and (14) for the cases $n = 1$ and $n = 2$. We need consider only the region $x \geq 0$ as we have imposed initial conditions which are symmetric about $x = 0$. To solve the equations we apply the boundary conditions $\partial\alpha/\partial x = \partial\beta/\partial x = \partial\gamma/\partial x = 0$ at $x = 0$ and we note that there will be another symmetrically disposed solution in the region $x \leq 0$. We apply no flux boundary conditions at some large value of x, typically $x = 500$, as the system will tend to its unreacted spatially uniform state at large distances from the origin. The numerical scheme used is the method of lines. We discretise in x by replacing the spatial derivatives with second order central-difference approximations. This gives the three sets of ordinary differential equations,

$$\frac{\partial\alpha_i}{\partial\tau} = \frac{1}{(\Delta x)^2}\left[\alpha_{i+1} - 2\alpha_i + \alpha_{i-1}\right] + \mu e^{-\epsilon_0\delta\tau} - \alpha_i\beta_i^n, \tag{19}$$

$$\frac{\partial\beta_i}{\partial\tau} = \frac{1}{(\Delta x)^2}\left[\beta_{i+1} - 2\beta_i + \beta_{i-1}\right] + \alpha_i\beta_i^n - \frac{m}{\delta}\beta_i^m\gamma_i, \tag{20}$$

$$\frac{\partial\gamma_i}{\partial\tau} = \frac{1}{(\Delta x)^2}\left[\gamma_{i+1} - 2\gamma_i + \gamma_{i-1}\right] - \frac{1}{\delta}\beta_i^m\gamma_i, \tag{21}$$

for $i = 0, 1, 2, 3, ..., N$ and where α_i, β_i and γ_i represent the values of α, β and γ at time τ and distance $i\Delta x$ from the origin. The outer boundary conditions are given as $\alpha_{N-1} = \alpha_{N+1}$, $\beta_{N-1} = \beta_{N+1}$, $\gamma_{N-1} = \gamma_{N+1}$ and similarly the boundary conditions at the origin are $\alpha_{-1} = \alpha_1$, $\beta_{-1} = \beta_1$, $\gamma_{-1} = \gamma_1$. To solve the above set of coupled nonlinear ordinary differential equations we used the NAG DO2BBF fourth-order Runge Kutta scheme. A spatial step size of $\Delta x = 0{\cdot}025$ was used and the Runge-Kutta scheme had a variable step size. It was necessary to use a scheme which was fourth-order accurate in time to capture the rapid growth in concentration, characteristic of clock-reaction behaviour. When the spatial step size was halved the results remained consistent to within the excepted accuracy of the scheme. The outer boundary conditions were applied at large distances from the origin so that the propagating wave profile could be given sufficient time to develop.

The solutions for the cases $n = 1$ and $n = 2$ display very similar characteristics and so we present the two sets of results together. Figure 1 shows how the concentration of the autocatalyst varies during the early stages of the reaction. At $\tau = 0$ the concentration of the autocatalyst, β, is zero everywhere apart from a unit step function of half width ξ about the origin. As the reaction proceeds, diffusion smooths out the initial step function in the neighbourhood of $x = \xi$ and a spatially uniform decay occurs in the vicinity of the origin. The autocatalyst is consumed because it reacts with the inhibitor chemical. At later times the distinction is lost between the region of spreading and that of spatially uniform decay. The autocatalyst continues to decrease in concentration and remains monotonically decreasing from its maximum at the origin to zero at infinity.

We now enter the induction period where the autocatalyst concentration remains small and inhibitor from outside the region $|x| < \xi$ diffuses inwards to replace consumed inhibitor. The concentration α continues to increase everywhere because of the decay of the precursor chemical. At some time later the autocatalyst concentration stops decreasing and starts to grow. Inhibitor chemical is consumed in the region around the origin and there is then a very rapid growth in the concentration β and a corresponding decrease in the concentration α. The rapid growth in autocatalyst concentration is illustrated in Figure 2.

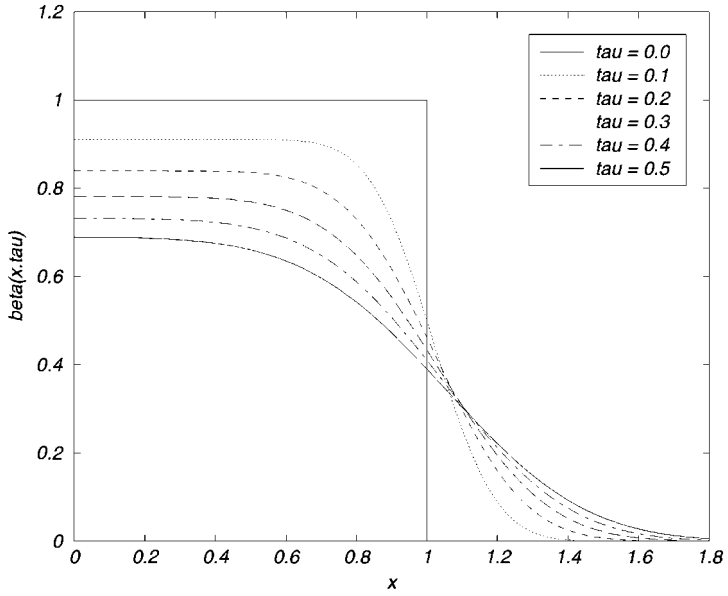

Figure 1. Initial decay of the autocatalyst for the case $n = 2$ with $\mu = 5$, $\lambda = 1$, $\epsilon_0 = 1$, $\xi = 1$ and $\delta = 0{\cdot}2$.

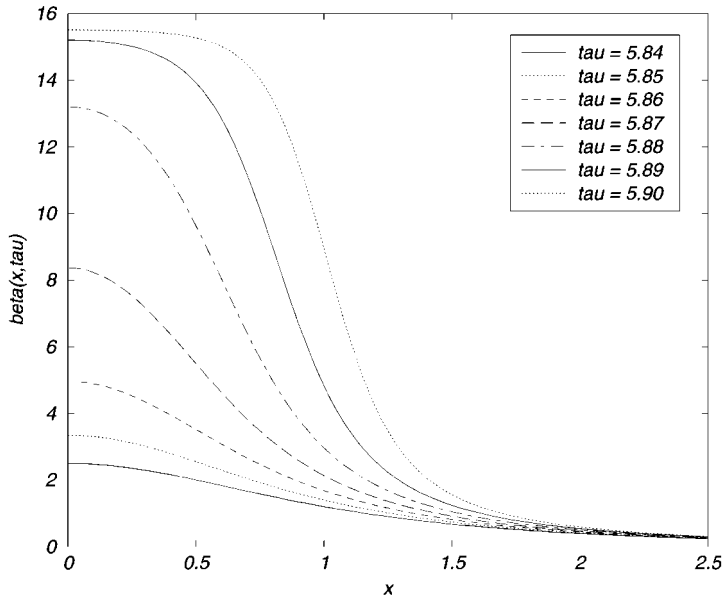

Figure 2. Rapid growth of the autocatalyst for the case $n = 2$ with $\mu = 5$, $\lambda = 1$, $\epsilon_0 = 1$, $\xi = 1$ and $\delta = 0{\cdot}2$.

At approximately $\tau = 5{\cdot}9$ we begin to observe the development of a wave indicated by a spatially uniform region in the vicinity of the origin followed by a sharp decay in β. Behind the profile we find that the concentration of the inhibitor chemical and chemical A have decayed to become very small.

The evolution of the wave profile for the case $n = 2$ is shown in Figure 3. For reasons of clarity we have shown only the autocatalyst concentrations. The wave profile is observed to both propagate away from the origin and grow as time increases. The growth corresponds to an increase in the concentration of the autocatalyst behind the wave and an increase in the

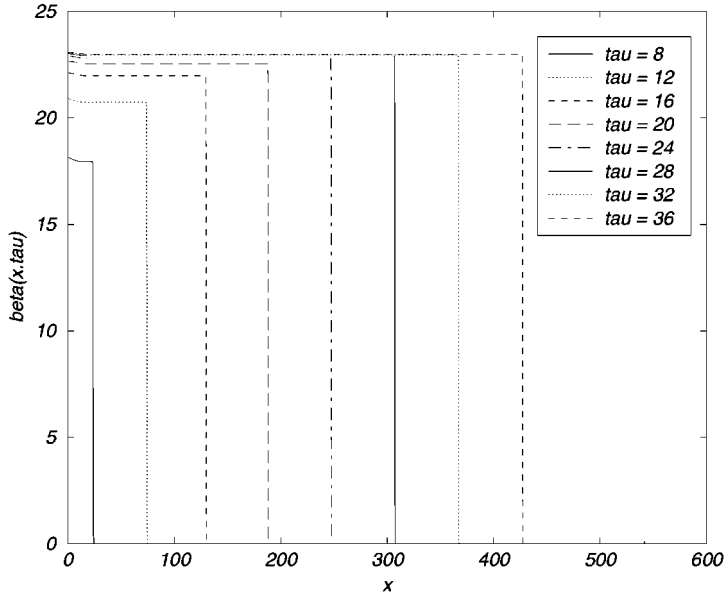

Figure 3. The evolution of the reaction-diffusion front for the case $n = 2$ with $\mu = 5$, $\lambda = 1$, $\epsilon_0 = 1$, $\xi = 1$ and $\delta = 0{\cdot}2$.

concentration of A in front of the wave. The increase in α in front of the wave is due to the decay of the precursor and behind the wave A reacts with B via autocatalysis to produce more B, hence β also increases. Once the precursor chemical has decayed fully, the growth of the wave stops and we find that the wavefront travels the same distance during each period of four time units, indicating that it is travelling with constant speed.

Figures 4 and 5 show the structure of fully developed travelling-wave profiles for the cases $n = 1$ and $n = 2$, respectively. Behind the wavefront all the inhibitor has been consumed and the system is in a fully reacted state. Ahead of the wavefront the solution is in an unreacted state with $\beta = 0$, $\gamma = \lambda$ and α being a spatially uniform constant which tends towards $\mu/(\epsilon_0\delta)$ as the decay of the precursor continues. All the reaction processes are taking place in the centred region whose boundary is propagating away from the origin. We note that the width of the region for the case $n = 1$ is considerably larger than for the case $n = 2$.

To investigate the speed of the wave profile it was necessary to determine the position of the front at each time step. This was defined to be the value of x at which $\partial\beta/\partial x$ took its minimum value. By considering the position of the wavefront at time τ and the position two time increments earlier, $\tau - 2\Delta\tau$, the wave speed was calculated via a central-difference approximation. A value of $\Delta\tau = 0{\cdot}25$ was used throughout. The results for the cases $n = 1$ and $n = 2$ are shown in Figures 6 and 7, respectively.

The intersection of the curve with the horizontal axis marks the end of the induction period and there is then a sharp jump associated with the initiation of the reaction-diffusion front. The wave speed is then seen to increase to its maximum value.

For the case $n = 1$ the numerical results suggest that the final steady wave speed varies like $\delta^{-1/2}$ but for the case $n = 2$ the they suggest the final wave speed to vary like δ^{-1}. In the asymptotic analysis we show that these assumptions must be made for us to construct asymptotic solutions.

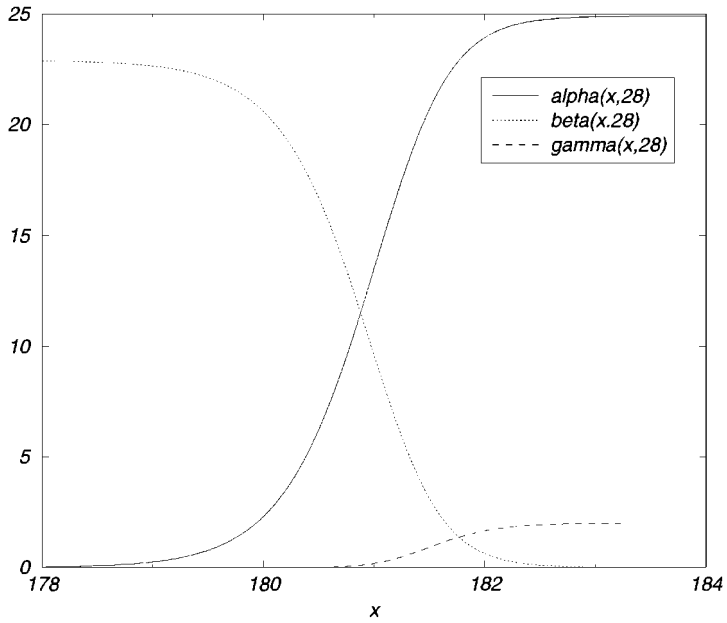

Figure 4. Travelling-wave profile for the case $n = 1$ with $\mu = 5$, $\lambda = 2$, $\epsilon_0 = 1$, $\xi = 1$ and $\delta = 0{\cdot}2$.

We note that the numerical results indicate that a constant-speed travelling-wave is observed only once the precursor has fully decayed. This implies that the concentration of chemical A ahead of the wave is the factor which controls the speed of the wave. Such results have also been found by Merkin and Needham [15] who studied a similar system which had a decay step instead of an inhibition step.

4. Travelling-wave analysis

After initiation of the reaction-diffusion front the numerical solution suggests that the governing equations will admit a solution of the form,

$$y = x - \sigma(\tau). \tag{22}$$

For small times after the end of the induction period, Figure 3 indicates that $\sigma = O(\tau^p)$, where $n > p$. Indeed, it has been shown by Merkin and Needham [15] that, for a cubic autocatalytic system which has a decay step rather than an inhibition step, the wavefront is an $O(\tau^2)$ distance away from the origin when the precursor chemical is assumed to decay slowly. Further investigation shows that the governing equations have a constant-speed travelling-wave solution when the precursor concentration become small, that is that $\sigma = O(\tau)$ when $e^{-\epsilon_0 \delta \tau} \ll 1$. In this limit both the concentration of chemical A ahead of the front and the concentration of the autocatalyst behind the front become constant, as shown in Figures 4 and 5. We now analyse the behaviour of the system in this limit and fix the similarity variable y as,

$$y = x - c\tau, \tag{23}$$

where c is the constant speed of the propagating reaction-diffusion front.

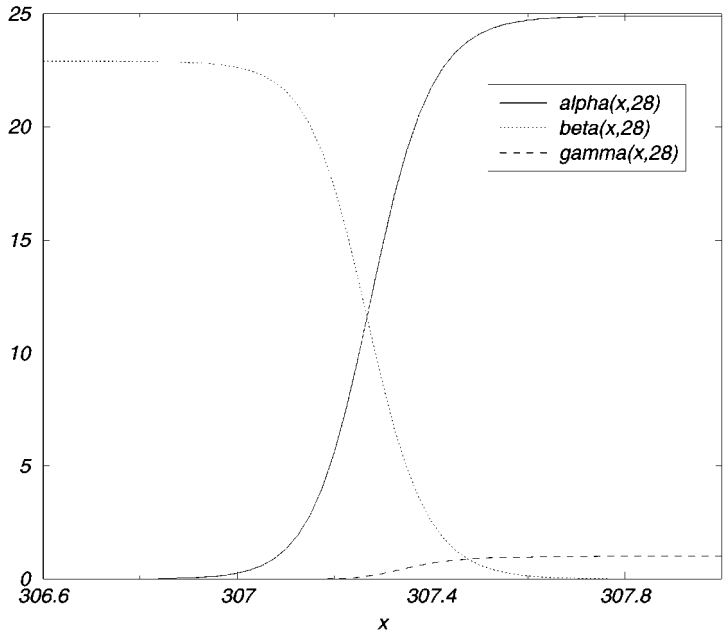

Figure 5. Travelling-wave profile for the case $n = 2$ with $\mu = 5$, $\lambda = 1$, $\epsilon_0 = 1$, $\xi = 1$ and $\delta = 0{\cdot}2$.

4.1. Formulation of the travelling-wave problem

If we neglect the input of A from the precursor chemical and apply the change of variables (23) then Equations (12), (13) and (14) become,

$$\alpha_{yy} + c\alpha_y - \alpha\beta^n = 0, \tag{24}$$

$$\beta_{yy} + c\beta_y + \alpha\beta^n - \frac{1}{\delta}\beta^n\gamma = 0, \tag{25}$$

$$\gamma_{yy} + c\gamma_y - \frac{n}{\delta}\beta^n\gamma = 0, \tag{26}$$

where subscript y denotes differentiation with respect to y, the travelling-wave coordinate. For the purpose of this analysis we assume that the parameters λ and μ are of $O(1)$. The boundary conditions ahead of the wave are those of the unreacted state: there is no autocatalyst present, the concentration of the inhibitor is constant and α has grown to its maximum value via precursor decay so that,

$$\alpha \to \frac{\mu}{\epsilon_0\delta}, \quad \beta \to 0, \quad \gamma \to \lambda, \tag{27}$$

as $y \to \infty$. Figures 4 and 5 show fully developed constant-speed travelling waves. It can be seen that ahead of the travelling waves, condition (27) is satisfied and that behind the wavefronts both the concentrations α and γ are small, possibly zero, and β takes a constant value. If we now consider the variable ϕ defined as,

$$\phi = \alpha + \beta - n\gamma, \tag{28}$$

then addition of Equations (24), (25) and (26) shows ϕ to satisfy the ordinary differential equation,

$$\phi_{yy} + c\phi_y = 0. \tag{29}$$

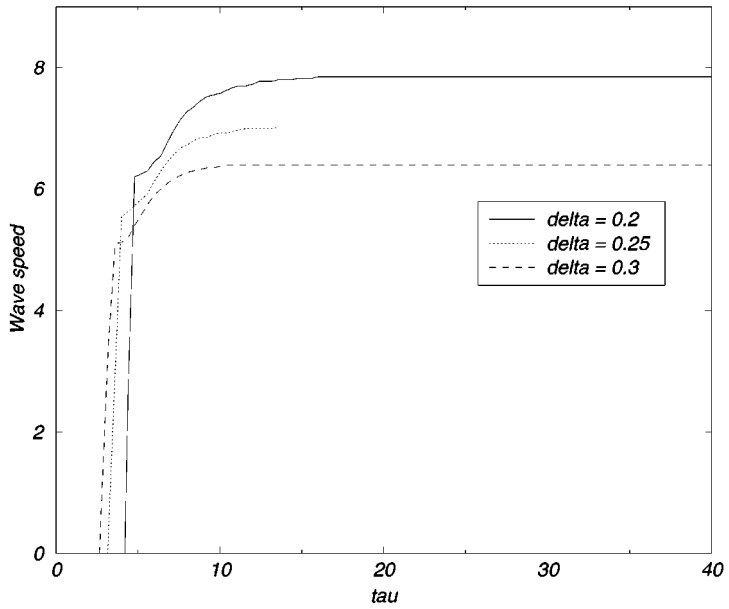

Figure 6. Wave Speed as a function of time for the case $n = 1$ with $\mu = 5$, $\lambda = 2$, $\epsilon_0 = 1$, $\xi = 1$ and $\delta = 0{\cdot}2,\ 0{\cdot}25,\ 0{\cdot}3$

Applying the boundary conditions as $y \to \infty$ we obtain,

$$\phi = \frac{\mu}{\epsilon_0 \delta} - n\lambda. \tag{30}$$

Equations (24), (25) and (26) show that for steady-state conditions both α and γ must be zero for β non-zero, hence from (28) and (30) we deduce the conditions behind the wave to be,

$$\alpha \to 0, \quad \beta \to \frac{\mu}{\epsilon_0 \delta} - n\lambda, \quad \gamma \to 0, \tag{31}$$

as $y \to -\infty$. We are now able to eliminate γ from Equation (25) and thus obtain the fourth-order system,

$$\alpha_{yy} + c\alpha_y - \alpha\beta^n = 0, \tag{32}$$

$$\beta_{yy} + c\beta_y + \alpha\beta^n - \frac{n}{\delta}\beta^n\left(\alpha + \beta - \frac{k}{\delta}\right) = 0, \tag{33}$$

subject to the boundary conditions,

$$\alpha \to \frac{k}{\delta} + n\lambda, \quad \beta \to 0, \qquad y \to \infty, \tag{34}$$

$$\alpha \to 0, \quad \beta \to \frac{k}{\delta}, \qquad y \to -\infty, \tag{35}$$

where

$$k = \frac{\mu}{\epsilon_0} - \delta n\lambda. \tag{36}$$

As this system is four dimensional it is difficult to use phase-space techniques. In the following sections we present asymptotic solutions valid for $\delta \ll 1$ for both cases. To construct

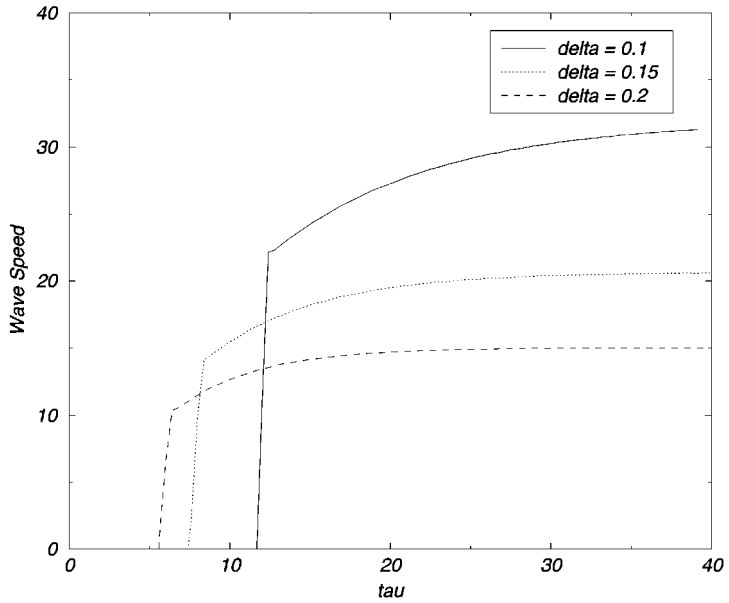

Figure 7. Wave speed as a function of time for the case $n = 2$ with $\mu = 5$, $\lambda = 1$, $\epsilon_0 = 1$, $\xi = 1$ and $\delta = 0{\cdot}1,\ 0{\cdot}15,\ 0{\cdot}2$.

these solutions we use information from the numerical solution of the initial-boundary-value problem to pose suitable expansions for the wave speed.

4.2. Quadratic autocatalysis with linear inhibition ($n = 1$)

Solutions are required to Equations (32) and (33) with $n = 1$ subject to boundary conditions (34) and (35), where k is defined as,

$$k = \frac{\mu}{\epsilon_0} - \delta\lambda. \tag{37}$$

The results in Figure 6 suggest that the final wave speed is of $O(\delta^{-\frac{1}{2}})$, hence we pose an expansion of the form,

$$c = \frac{c_0}{\delta^{1/2}} + c_1 + o(1). \tag{38}$$

The structure of the small-δ asymptotic solution is shown schematically in Figure 8 and can been seen to consist of four asymptotic regions. Behind the wavefront, exponentially small corrections to the boundary condition are constructed. When developed, these solutions show the need for a further asymptotic region in which both α and β are of $O(\delta^{-1})$. Consideration of the system ahead of the wave also shows corrections to the boundary condition to be exponentially small. A further asymptotic region is then required to link these solutions into the central asymptotic region, region II, in which both α and β are of $O(\delta^{-1})$. This central region has width of $O(\delta^{\frac{1}{2}})$ and contains the equation for the travelling-wave solution the Fisher problem at leading order. We now give a description of the asymptotic structure of the full solution.

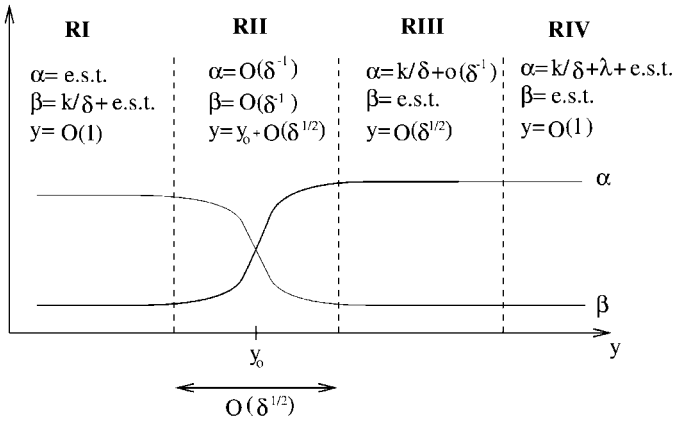

Figure 8. Schematic diagram showing the asymptotic structure of the travelling-wave solution for the case $n = 1$. Exponentially small terms have been denoted by e.s.t.

Region I:
For consistent asymptotic expansions to be developed we require exponentially small corrections to boundary conditions (35). Appropriate scalings are thus,

$$\bar{\alpha} = \delta^{\frac{1}{2}} \log \alpha = O(1), \quad \bar{\beta} = \delta^{\frac{1}{2}} \log \left(\frac{k}{\delta} - \beta \right) = O(1), \quad y = \bar{y} = O(1), \tag{39}$$

and by assuming appropriate expansions we obtain, in terms of the unscaled variables, the solutions

$$\alpha = A(\delta) \exp \left(\frac{\nu y}{\delta^{\frac{1}{2}}} - \frac{c_1 \nu y}{2\nu + c_0} \right) \left(1 + o(1) \right), \tag{40}$$

$$\beta = \frac{k}{\delta} - A(\delta) \exp \left(\frac{\nu y}{\delta^{\frac{1}{2}}} - \frac{c_1 \nu y}{2\nu + c_0} \right) \left(1 + o(1) \right), \tag{41}$$

where ν is given by,

$$\nu = -\frac{c_0}{2} + \frac{\sqrt{c_0^2 + 4k}}{2}, \tag{42}$$

and $A(\delta)$ is a constant of integration. Expansion (41) becomes non-uniform when the exponentially small term grows to become of $O(\delta^{-1})$. This occurs when,

$$y = \frac{\delta^{1/2}}{\nu} \log \left(\frac{1}{\delta A(\delta)} \right), \tag{43}$$

and suggests that a new asymptotic region is required in which both α and β are of $O(\delta^{-1})$.

We now construct a solution in the region ahead of the reaction front.

Region IV:
It is not immediately obvious what form the scalings should take for this region so we pose an asymptotic expansion of the form,

$$\alpha = \frac{k}{\delta} + \lambda + \tilde{\alpha} + \cdots, \quad \beta = \tilde{\beta} + \cdots, \tag{44}$$

with $y = \tilde{y} = O(1)$ and where $\tilde{\alpha} \ll 1$ and $\tilde{\beta} \ll 1$. If we now substitute in Equations (32) and (33) and linearise we obtain,

$$\tilde{\alpha}_{\tilde{y}\tilde{y}} + \left(\frac{c_0}{\delta^{1/2}} + c_1\right)\tilde{\alpha}_{\tilde{y}} - \left(\frac{k}{\delta} + \lambda\right)\tilde{\beta} \sim 0, \tag{45}$$

$$\tilde{\beta}_{\tilde{y}\tilde{y}} + \left(\frac{c_0}{\delta^{1/2}} + c_1\right)\tilde{\beta}_{\tilde{y}} + \left(\frac{k}{\delta} + \lambda\right)\tilde{\beta} - \frac{\lambda}{\delta}\tilde{\beta} \sim 0. \tag{46}$$

Equation (46) has a solution of the form,

$$\tilde{\beta} \sim \tilde{b}_1(\delta)\exp\left(\frac{\theta_+\tilde{y}}{\delta^{1/2}}\right) + \tilde{b}_2(\delta)\exp\left(\frac{\theta_-\tilde{y}}{\delta^{1/2}}\right), \tag{47}$$

where $\tilde{b}_1$ and $\tilde{b}_2$ are gauge functions and,

$$\theta_\pm = \frac{1}{2}\left(-c_0 \pm \sqrt{c_0^2 - 4(k-\lambda)}\right). \tag{48}$$

Substituting this result in Equation (45) and solving we have,

$$\begin{aligned}\tilde{\alpha} \;\sim\; & \tilde{a}_1(\delta) + \tilde{a}_2(\delta)\exp\left(\frac{-c_0\tilde{y}}{\delta^{1/2}}\right) \\ & + \frac{\left(\frac{k}{\delta} + \lambda\right)\tilde{b_1}(\delta)\exp\left(\frac{\theta_+\tilde{y}}{\delta^{1/2}}\right)}{\left(\frac{\theta_+^2}{\delta} + \frac{c_0\theta_+}{\delta}\right)} + \frac{\left(\frac{k}{\delta} + \lambda\right)\tilde{b_2}(\delta)\exp\left(\frac{\theta_-\tilde{y}}{\delta^{1/2}}\right)}{\left(\frac{\theta_-^2}{\delta} + \frac{c_0\theta_-0}{\delta}\right)}.\end{aligned} \tag{49}$$

We note that the gauge functions $\tilde{a}_1(\delta)$, $\tilde{a}_2(\delta)$, $\tilde{b}_1(\delta)$ and $\tilde{b}_2(\delta)$ are completely undetermined at present. Consideration of Equation (49) shows that when $\tilde{y} = O(\delta^{1/2})$ expansions (44) may become non-uniform. We now choose to examine the behaviour of the solution in this limit by considering the scaled variable,

$$\tilde{y} = \delta^{1/2}\breve{y}. \tag{50}$$

Rewriting the governing equations in terms of the variable $\breve{y}$ we obtain,

$$\frac{\alpha_{\breve{y}\breve{y}}}{\delta} + \left(\frac{c_0}{\delta^{1/2}} + c_1\right)\frac{\alpha_{\breve{y}}}{\delta^{1/2}} - \alpha\beta = 0, \tag{51}$$

$$\frac{\beta_{\breve{y}\breve{y}}}{\delta} + \left(\frac{c_0}{\delta^{1/2}} + c_1\right)\frac{\beta_{\breve{y}}}{\delta^{1/2}} + \alpha\beta - \frac{\beta}{\delta}\left(\alpha + \beta - \frac{k}{\delta}\right) = 0. \tag{52}$$

If we now pick all the gauge functions, $\tilde{a}_1(\delta)$, $\tilde{a}_2(\delta)$, $\tilde{b}_1(\delta)$ and $\tilde{b}_2(\delta)$, to be $O(1)$, then we find that appropriate expansions are,

$$\alpha = \frac{k}{\delta} + \breve{\alpha} + o(1), \quad \beta = \breve{\beta} + o(1). \tag{53}$$

To examine these new scalings we introduce a further asymptotic region.

Region III

Again the exact form of the scalings is not clear at present so we pose expansions (53) and scale y as,

$$y = \delta^{1/2}\breve{y}. \tag{54}$$

Equations (32) and (33) become, at leading order,

$$\breve{\alpha}_{\breve{y}\breve{y}} + c_0\breve{\alpha}_{\breve{y}} - k\breve{\beta} = 0, \tag{55}$$

$$\breve{\beta}_{\breve{y}\breve{y}} + c_0\breve{\beta}_{\breve{y}} + k\breve{\beta} - \breve{\beta}(\breve{\alpha} + \breve{\beta}) = 0. \tag{56}$$

These equations admit solutions of the form (47) and (49) and hence match with the solutions in region IV as $\breve{y} \to \infty$. It is not possible to obtain fully analytical solutions of Equations (55) and (56) valid for all $\breve{y}$, so we try to obtain the behaviour of the system as $\breve{y} \to -\infty$. Equations (55) and (56) linearise if we choose $\breve{\alpha} = -\breve{\beta}$ and the resulting system is easily solved to give,

$$\breve{\alpha} = -\breve{b}_1 e^{\zeta_+ \breve{y}} - \breve{b}_2 e^{\zeta_- \breve{y}}, \tag{57}$$

$$\breve{\beta} = \breve{b}_1 e^{\zeta_+ \breve{y}} + \breve{b}_2 e^{\zeta_- \breve{y}}, \tag{58}$$

where,

$$\zeta_\pm = -\frac{1}{2}\left(c_0 \pm \sqrt{c_0^2 - 4k}\right). \tag{59}$$

We now show, via a numerical integration, that this is the behaviour of Equations (55) and (56) as $\breve{y} \to -\infty$. We accomplished the integration by discretising the two equations with respect to $\breve{y}$ and then solving the resulting set of nonlinear equations using the NAG routine C05NBF. To obtain boundary conditions as $\breve{y} \to \infty$ we use the matching conditions from region IV and fix,

$$\breve{\alpha} = \lambda, \quad \breve{\beta} = 0, \tag{60}$$

hence we neglect terms which are exponentially small. As $\breve{y} \to -\infty$ we ensure that the solution is of the linearised form discussed above and fix,

$$\breve{\alpha} = -e^{\zeta_+ \breve{y}} - \breve{b}_2 e^{\zeta_- \breve{y}}, \tag{61}$$

$$\breve{\beta} = e^{\zeta_+ \breve{y}} + \breve{b}_2 e^{\zeta_- \breve{y}}. \tag{62}$$

The travelling-wave solution is invariant under a shift in the travelling-wave coordinate, y, so we can set $\breve{b}_1 = 1$ for the purpose of our numerical solution. Different values of the parameters were used, within the parameter regime $c_0 > 2\sqrt{k}$ which ensures that $\zeta_\pm$ is real, and the scheme was found to converge each time. Changing the point at which the solution was truncated had no effect on the overall solution. Figure 9 shows such a solution of Equations (55) and (56) subject to the boundary conditions described above. It can be observed that $\breve{\alpha}$ and $\breve{\beta}$ decay from being exponentially large as $\breve{y} \to -\infty$ to become λ and 0, respectively, as $\breve{y} \to \infty$. We conclude that the linearised behaviour of Equations (55) and (56) is the behaviour as $y \to -\infty$. In terms of the original variables these linearised solutions are written as,

$$\alpha \sim k - \breve{b}_1 e^{\zeta_+ y/\delta^{1/2}} - \breve{b}_2 e^{\zeta_- y/\delta^{1/2}}, \tag{63}$$

$$\beta \sim \breve{b}_1 e^{\zeta_+ y/\delta^{1/2}} + \breve{b}_2 e^{\zeta_- y/\delta^{1/2}}. \tag{64}$$

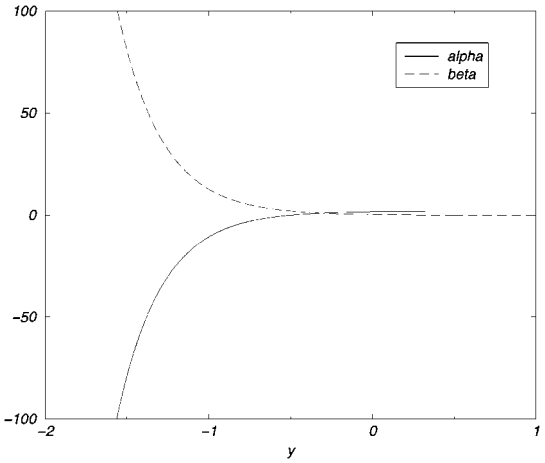

Figure 9. Numerical solution of Equations (55) and (56).

Expansion (63) becomes non-uniform as $y \to -\infty$ in particular when,

$$\breve{y} = -\frac{\delta^{1/2}}{\zeta_+} \log \delta. \tag{65}$$

This suggests a new region in which α and β are $O(\delta^{-1})$.

Region II:
This region is the central region and matches to region III as $\hat{y} \to \infty$ and region I as $\hat{y} \to -\infty$. Appropriate scalings are,

$$\hat{\alpha} = \delta\alpha = O(1), \quad \hat{\beta} = \delta\beta = O(1), \quad \hat{y} = \frac{y - y_0(\delta)}{\delta^{1/2}} = O(1). \tag{66}$$

For consistent matching $y_0(\delta)$ must be the same when evaluated in region I and in region III, giving the relation,

$$y_0(\delta) = -\frac{\delta^{1/2}}{\nu} \log [\delta A(\delta)] = -\frac{\delta^{1/2}}{\zeta_+} \log \delta, \tag{67}$$

must be satisfied. Under scalings (66) Equations (32) and (33) become,

$$\hat{\alpha}_{\hat{y}\hat{y}} + \left(c_0 + \delta^{1/2} c_1\right) \hat{\alpha}_{\hat{y}} - \hat{\alpha}\hat{\beta} = 0, \tag{68}$$

$$\hat{\beta}_{\hat{y}\hat{y}} + \left(c_0 + \delta^{1/2} c_1\right) \hat{\beta}_{\hat{y}} + \hat{\alpha}\hat{\beta} - \hat{\beta}\left(\frac{\hat{\alpha}}{\delta} + \frac{\hat{\beta}}{\delta} - \frac{k}{\delta}\right) = 0, \tag{69}$$

which at leading order take the form,

$$\hat{\alpha}_{0_{\hat{y}\hat{y}}} + c_0 \hat{\alpha}_{0_{\hat{y}}} - \hat{\alpha}_0 \hat{\beta}_0 = 0, \tag{70}$$

$$\hat{\alpha}_0 + \hat{\beta}_0 = k. \tag{71}$$

Elimination of $\hat{\alpha}_0$ gives the two-dimensional system,

$$\hat{\beta}_{0_{\hat{y}\hat{y}}} + c_0 \hat{\beta}_{0_{\hat{y}}} - \hat{\beta}_0 \left(\hat{\beta}_0 - k\right) = 0, \tag{72}$$

Table 1. Comparison of the analytical minimum wave speed and the numerical estimate for the case $n = 1$ with $\mu = 5$, $\lambda = 2$, $\epsilon_0 = 1$ and $\xi = 1$.

δ	Numerical estimate of the wave speed	Analytical minimum wave speed
0·2	7·8	9·6
0·25	7·0	8·5
0·3	6·4	7·7

subject to the boundary conditions,

$$\hat{\beta}_0 \to k, \quad \hat{y} \to -\infty, \qquad \hat{\beta}_0 \to 0, \quad \hat{y} \to +\infty. \tag{73}$$

The parameter k can be removed from Equation (72) and boundary conditions (73) by appropriately scaling $\hat{\beta}_0$, c_0 and $\hat{y}$ Dropping hats and subscripts we obtain the equation,

$$\beta_{yy} + c_0\beta_y + \beta(1-\beta) = 0, \tag{74}$$

subject to the conditions,

$$\beta \to 1, \quad y \to -\infty, \qquad \beta \to 0, \quad y \to +\infty. \tag{75}$$

Equation (74) is the equation for the travelling-wave solution of Fisher's Equation [2] which has been rigorously analysed by Kolmogorov *et al.* [3]. It is well known that a minimum-wave-speed solution exists and this has been shown by Larson [16] to be the solution which will develop from compact-support initial conditions. In terms of our original variables the minimum wave speed is given as,

$$C_{\min} = 2\left(\frac{\mu}{\epsilon_0\delta} - \lambda\right)^{1/2} + O(1). \tag{76}$$

Table 1 shows that agreement is observed to within the expected $O(1)$ accuracy between the numerical and asymptotic solution.

This completes the asymptotic solution for $\delta \ll 1$. We have shown that solutions which consist of exponentially small corrections to the boundary conditions can be developed to give a central region in which both $\alpha = O(\delta^{-1})$ and $\beta = O(\delta^{-1})$. Within this region we obtain the equation for the travelling-wave solution of the standard Fisher problem at leading order which fixes a minimum wave speed.

4.3. Cubic autocatalysis with quadratic inhibition ($n = 2$)

Solutions are required to Equations (32) and (33) with $n = 2$ subject to boundary conditions (34) and (35), where k is defined as,

$$k = \frac{\mu}{\epsilon_0} - 2\delta\lambda. \tag{77}$$

Figure 7 shows a plot of wave speed vs time for three different values of δ. These results indicate that the final wave speed is of $O(\delta^{-1})$ hence we pose an expansion of the form,

$$c = \frac{c_0}{\delta} + c_1 + o(1). \tag{78}$$

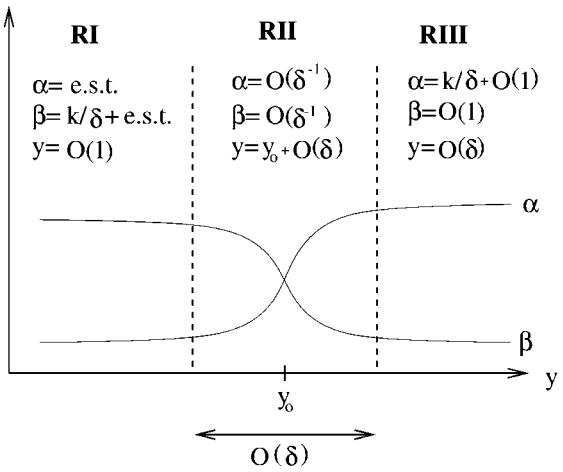

Figure 10. Schematic diagram showing the asymptotic structure of the travelling-wave solution for the case $n = 2$. Exponentially small terms have been denoted by e.s.t.

The structure of the small-δ asymptotic solution is shown schematically in Figure 10 and can been seen to consist of three asymptotic regions. Behind the wavefront exponentially small corrections to the boundary conditions are constructed. When developed these solutions show the need for a further asymptotic region in which both α and β are $O(\delta^{-1})$. Ahead of the wavefront, exponential corrections are again developed which again suggest a central region of width $O(\delta)$ in which α and β are of $O(\delta^{-1})$. The central region contains the equation for the travelling-wave solution of the cubic Fisher problem at leading order. We now give a brief description of the asymptotic structure.

Region I:
Appropriate scalings require exponentially small corrections to the boundary conditions behind the wave. These are,

$$\bar{\alpha} = \delta \log \alpha = O(1), \quad \bar{\beta} = \log\left(\frac{k}{\delta} - \beta\right) = O(1), \quad y = \bar{y} = O(1). \tag{79}$$

By posing suitable expansions we obtain, in terms of the unscaled variables, the expansions,

$$\alpha = A(\delta) \exp\left(\frac{\nu y}{\delta} - \frac{c_1 \nu y}{(2\nu + c_0)}\right)\left(1 + o(1)\right), \tag{80}$$

$$\beta = \frac{k}{\delta} - A(\delta) \exp\left(\frac{\nu y}{\delta} - \frac{c_1 \nu y}{(2\nu + c_0)} +\right)\left(1 + o(1)\right), \tag{81}$$

where

$$\nu = -\frac{c_0}{2} + \frac{\sqrt{c_0^2 + 4k^2}}{2}, \tag{82}$$

and $A(\delta)$ is a constant of integration. Non-uniformities occur when,

$$y = \frac{\delta}{\nu} \log\left(\frac{1}{\delta A(\delta)}\right). \tag{83}$$

Region III:
We now construct a solution in the region ahead of the reaction front. To obtain balances at leading order we choose the scalings,

$$\tilde{\alpha} = \alpha - \frac{k}{\delta} = O(1), \quad \tilde{\beta} = \beta = O(1), \quad \tilde{y} = \frac{y}{\delta} = O(1). \tag{84}$$

In terms of unscaled variables we obtain,

$$\alpha = \frac{k}{\delta} + 2\lambda - a(\delta)\mathrm{e}^{-c_0 y/\delta}, \tag{85}$$

$$\beta = a(\delta)\mathrm{e}^{-c_0 y/\delta}. \tag{86}$$

From these expansions we observe that non-uniformities will occur as $y \to -\infty$ in particular when,

$$y = -\frac{\delta}{c}\log\left[\frac{1}{a(\delta)}\right]. \tag{87}$$

Again, this suggests a central region of width $O(\delta)$ in which both α and β are of $O(\delta^{-1})$.

Region II:
This central region matches to region I as $y \to -\infty$ and to region III as $y \to \infty$. Appropriate scalings are,

$$\hat{\alpha} = \delta\alpha = O(1), \quad \hat{\beta} = \delta\beta = O(1) \quad \text{and} \quad \hat{y} = \frac{y - y_0}{\delta} = O(1), \tag{88}$$

which when substituted in the governing equations give the leading-order balances,

$$\hat{\alpha}_0 + \hat{\beta}_0 = k, \tag{89}$$

$$\hat{\alpha}_{0\hat{y}\hat{y}} + c_0\hat{\alpha}_{0\hat{y}} - \hat{\alpha_0}\hat{\beta_0}^2 = 0. \tag{90}$$

Elimination of $\hat{\alpha}_0$ gives the second-order equation,

$$\hat{\beta}_{0\hat{y}\hat{y}} + c_0\hat{\beta}_{0\hat{y}} + \hat{\beta}_0^2(k - \hat{\beta}_0) = 0 \tag{91}$$

subject to the boundary conditions,

$$\hat{\beta}_0 \to k, \quad \hat{y} \to -\infty \qquad \hat{\beta}_0 \to 0, \quad \hat{y} \to \infty. \tag{92}$$

The parameter k can be removed from Equation (91) and boundary conditions (92) by an appropriate scaling and, dropping hats and subscripts, we obtain the equation,

$$\beta_{yy} + c_0\beta_y + \beta^2(1 - \beta) = 0 \tag{93}$$

subject to the boundary conditions,

$$\beta \to 1, \quad y \to -\infty, \quad \beta \to 0, \quad y \to \infty. \tag{94}$$

Equation (93) is the equation for the travelling-wave solution of the cubic Fisher problem and has been studied extensively by Gray, Showalter and Scott [17], Britton [18, pp. 102–108] and Billingham and Needham [19].

Table 2. Comparison of the analytical minimum wave speed and the numerical estimate for the case $n = 2$ with $\mu = 5$, $\lambda = 1$, $\epsilon_0 = 1$ and $\xi = 1$.

δ	Numerical estimate of the wave speed	Analytical minimum wave speed
0·1	31·3	33·9
0·15	20·6	22·2
0·2	15·0	16·3

As in the last section we would expect the numerical solution of the full initial-boundary-value problem to agree with the analytical prediction for the minimum wave speed. In terms of the original variables this is given as,

$$c_{\min} = \frac{1}{\sqrt{2}}\left(\frac{\mu}{\epsilon_0\delta} - 2\lambda\right) + O(1). \tag{95}$$

Table 2 shows that agreement between the numerical and asymptotic solution is observed to within the expected $O(1)$ accuracy.

At this point we note that an alternative region III can be constructed in which $y = O(1)$. In this case we obtain solutions for α and β which grow like $1/(y - y_0)$ as $y \to y_0$, where y_0 is a constant which can be fixed by matching. This form of solution matches to the non-minimum wave speed cubic Fisher solution in region II and illustrates an important difference between the solutions in the cases of quadratic and cubic autocatalysis. In the quadratic case all travelling wave solutions decay exponentially ahead of the wave. In contrast, for the case of cubic autocatalysis, only the minimum wave speed decays exponentially, all other solutions decaying algebraically as $y \to \infty$. The details of this alternative region have been omitted as we expect the large-time solution to have the minimum wave speed.

This completes the asymptotic solution for $\delta \ll 1$. We have constructed a three-region solution by developing correction terms to the boundary conditions. The central region has width of $O(\delta)$ and both $\alpha = O(\delta^{-1})$ and $\beta = O(\delta^{-1})$. Within this region we obtain the cubic Fisher problem at leading order and this fixes a minimum wave speed.

5. Conclusion

We have studied the model reaction scheme for the cases $n = 1$ and $n = 2$ allowing all the chemical species to diffuse in one-dimensional slab geometry. Fully numerical solutions have been given for both cases which are found to display similar features. Clock-reaction behaviour was found to be characterised by a very rapid growth of the autocatalyst in a thin region centred about the origin. At the end of the induction period a growing accelerating reaction-diffusion front was evolved. This was then seen to develop into a travelling-wave at constant speed.

Large-time constant-speed travelling-wave solutions have been constructed for both the cases $n = 1$ and $n = 2$ by means of small δ asymptotics. Four regions were required for the case $n = 1$ to describe the full travelling-wave solution. In the central asymptotic region it was found that the leading-order problem reduced to the Fisher equation, hence showing the existence of a family of travelling-wave solutions above a minimum wave speed. For the case $n = 2$ only three asymptotic regions were required. This time the central region was found

to contain the cubic Fisher problem at leading order, again fixing a minimum wave speed. In both cases the asymptotic prediction of the wave speed agreed well with that of the numerical solution.

References

1. R. Luther, Discovery and analysis of chemical waves. *Elektrochem.* 12 (1906) 596–610.
2. R. A. Fisher, The wave of advance of advantageous genes. *Ann. Eugenics* 7 (1937) 355–369.
3. A. N. Kolmogorov, I. Petrovsky and N. Piscounoff, Study of the diffusion equation with increase in the quantity of matter, with application to a biological problem. *Bull. Univ. Moscow Ser. Int. Sec A.* 1 (1937) 1–17.
4. J. H. Merkin, D. J. Needham and S. K. Scott, The development of travelling waves in a simple isothermal chemical system I. Quadratic autocatalysis with linear decay. *Proc. R. Soc. London* A 424 (1989) 187–209.
5. K. W. Watkins and R. Distefano, The arsenic(iii) sulfide clock reaction. *J. Chem. Education* 64 (1987) 255–257.
6. P. Jones K. B. and Oldham, The theory of the formaldehyde clock reaction. *J. Chem. Education* 40 (1963) 366–368.
7. J. L. Lambert and G. T. Fina, Iodine clock reaction-mechanisms. *J. Chem. Education* 61 (1984) 1037–1038.
8. P. Jones, M. L. Haggett and J. L. Longridge, The hydration of carbon dioxide - A double clock experiment. *J. Chem. Education* 41 (1964) 610–612.
9. A. Hanna, A. Saul, and K. Showalter, Detailed studies of propagating fronts in the iodate oxidation of arsenous acid. *J. Amer. Chem. Soc.* 104 (1982) 3838–3844.
10. D. O. Cooke, *Inorganic Reaction Mechanisms*. London: The Chemical Society (1979).
11. J. Billingham, and D. J. Needham, Mathematical-modeling of chemical clock reactions. I. Induction, inhibition and the iodate arsenous-acid reaction. *Proc. R. Soc. London* A 340 (1992) 669–591.
12. G. W. Burnet and H. W. Melville, Determination of velocity coefficients for polymerisation processes. *Proc. R. Soc. London* A 189 (1947) 456–480.
13. J. Billingham and D. J. Needham, Mathematical modeling of chemical clock reactions II. A class of autocatalytic clock reaction schemes. *J. Eng. Math.* 27 (1993) 113–145.
14. S. J. Preece. A. C. King and J. Billingham, Chemical clock reactions: The effect of precursor consumption. *J. Mat. Chem.* 26 (1999) 47–73.
15. J. H. Merkin and D. J. Needham, Reaction-diffusion in a simple pooled chemical system. *Dynam. Stab. Sys.* 4 (1989) 141–167.
16. D. A. Larson, Transient bounds and time-asymptotic behaviour of solutions to nonlinear equations of Fisher type. *SIAM J. Appl. Mat.* 34 (1978) 93–103.
17. P. Gray, K. Showalter and S. K. Scott, Propagating reaction-diffusion fronts with cubic autocatalysis: The effects of reversibility. *J. Chimie Physique* 84 (1987) 1329–1333.
18. N. F. Britton, *Reaction Diffusion Equations and their Application to Biology*. London: Academic Press (1986).
19. J. Billingham and D. J. Needham, A note on the properties of a family of travelling-wave solutions arising in cubic autocatalysis. *Dynam. Stab. Sys.* 6 (1991) 33–39.